

## Fabrication of Aromatic Polyimide Films Derived from Diisocyanate with Fluorinated Dianhydride

(Pembuatan Filem Polimida Aromatik Terhasil daripada Diisosiyanat dengan Dianhidrida Berfluorinat)

NAJAA MUSTAFFA<sup>1</sup>, TATSUO KANEKO<sup>2</sup>, KENJI TAKADA<sup>2</sup>, SUMANT DWIVEDI<sup>3</sup> & NADHRATUN NAIIM MOBARAK<sup>1,\*</sup>

<sup>1</sup>*Department of Chemical Sciences, Faculty of Science and Technology, Universiti Kebangsaan Malaysia, 43600 UKM Bangi, Selangor Darul Ehsan, Malaysia*

<sup>2</sup>*Energy and Environment Area, Graduate School of Advanced Science and Technology, Japan Advanced Institute of Science and Technology, 1-1 Asahidai, Nomi, Ishikawa 923-1292, Japan*

<sup>3</sup>*Department of Physics, Technical University of Denmark, Kongens Lyngby 2800, Denmark*

Received: 27 December 2022/Accepted: 5 April 2023

### ABSTRACT

The range of available structure combinations to synthesize polyimide (PI) makes it technically possible to have various universal methods of producing PI film. The molecular design, in which monomers used to synthesize PI are carefully selected to meet specific application requirements as it influenced the properties of PI films. This study aimed to outline the approach for film fabrication through the casting of highly organo-soluble polyimide derived from 4,4'-methylene diphenyl diisocyanate (MDI) with 4,4'-(hexafluoroisopropylidene) diphtalic anhydride (6FDA) in different heating treatments. The solution drop amount was tested in order to control the films colour uniformity. A flexible and less crystalline MDI-6FDA film with an average thickness of 93  $\mu\text{m}$  was successfully developed with a tensile strength of up to 57 MPa and an elongation at break of 5%. The resulting MDI-6FDA film also demonstrated good optical transparency ( $T_{500} = 69\%$ ) with a cut-off wavelength at 371 nm and high thermal resistance ( $T_5 = 574\text{ }^\circ\text{C}$ ) with a  $T_g$  temperature of up to 238  $^\circ\text{C}$ . The obtained film also shows good chemical resistance in methanol, ethanol, isopropanol, and tetrahydrofuran solvents. These outcomes serve as a guideline for the fabrication of polyimide films specifically derived from diisocyanate and dianhydride, with the potential advantages to be used in optical applications.

Keywords: Diisocyanate; flexible films; optical transparency; polyimide; tensile strength

### ABSTRAK

Kepelbagaian gabungan struktur yang tersedia untuk mensintesis poliimida secara teknikalnya telah mewujudkan kaedah yang pelbagai untuk menghasilkan filem PI. Reka bentuk molekul yang melibatkan pemilihan monomer yang digunakan dalam penyediaan PI dipilih dengan teliti, bagi memenuhi keperluan aplikasi tertentu kerana ia boleh mempengaruhi sifat filem PI. Kajian ini bertujuan untuk menggariskan pendekatan bagi fabrikasi filem melalui penuangan poliimida organo-larut yang diperolehi daripada 4,4'-metilena difenil diisosiyanat (MDI) dengan 4,4'-(heksafluoroisopropilidena) diftalik anhidrida (6FDA) dalam rawatan pemanasan berbeza. Jumlah titisan larutan telah diuji bagi mengawal keseragaman warna filem. Filem MDI-6FDA yang fleksibel dan kurang hablur dengan purata ketebalan 93  $\mu\text{m}$  berjaya dibangunkan dengan kekuatan tegangan sehingga 57 MPa dan pemanjangan memutus pada 5%. Filem MDI-6FDA yang terhasil juga menunjukkan kelutsinaran optik yang baik ( $T_{500} = 69\%$ ) dengan panjang gelombang terpenggal pada 371 nm dan ketahanan terma yang tinggi ( $T_5 = 574\text{ }^\circ\text{C}$ ) dengan suhu  $T_g$  sehingga 238  $^\circ\text{C}$ . Filem yang dihasilkan juga menunjukkan ketahanan kimia yang baik dalam pelarut metanol, etanol, isopropanol dan tetrahidrofurana. Keputusan ini berfungsi sebagai garis panduan dalam fabrikasi filem poliimida khususnya daripada diisosiyanat dan dianhidrida dengan kelebihan potensi untuk digunakan di dalam aplikasi optik.

Kata kunci: Diisosiyanat; filem fleksibel; kekuatan tegangan; kelutsinaran cahaya; poliimida

## INTRODUCTION

Aromatic polyimides (PIs) have been well recognized as a high-performance polymer due to their outstanding heat resistance, mechanical performance, good chemical resistance and excellent electrical properties. These materials have been widely used in the aerospace and electronics industries (Hyde & Smith 1995; Liaw et al. 2012). In most industrial applications, PI is typically used in the form of films. Depending on the application, optical transparency of PI films is of special importance, such as substrates in image display devices, flexible organic photovoltaics, orientation films and optical fibres (Hasegawa, Fujii & Wada 2018; Tapaswi & Ha 2019). However, most PIs film have a strong UV-visible absorption because of their intense yellow or brown colour, arises from the highly conjugated aromatic structures and charge-transfer (CT) interactions (Ando, Matsuura & Sasaki 1997; Hasegawa & Horie 2001). It is also important to note that, while aromatic PIs have been used in several commercial applications, most PIs are insoluble due to the rigid chain structure which lead to serious film processing difficulties and limits their use in some applications (Sadavarte et al. 2009).

Hence, great efforts have been expanded to develop advanced PI material with both good solubility and transparency while retaining their thermal stability and other excellent properties (Amutha, Tharakan & Sarojadevi 2015; Ghosh, Mistri & Banerjee 2015; Thiruvassagam et al. 2016; Wu, Li & Liu 2012). According to St Clair, St Clair and Shevket (1984), the presence of bulky electron-withdrawing group in the polymer backbone could lighten the colour of polymer films and enhance their processability. Recently, considerable attention has been devoted to the synthesis of fluorine containing polymers. Incorporation of the bulky fluorine groups serves to increase the free volume of the polymers, thereby improving properties like solubility and optical transparency (Deng et al. 2018; Liaw, Huang & Chen 2006; Qu et al. 2001). Therefore, in this study, 4,4'-(hexafluoroisopropylidene) diphthalic anhydride (6FDA) is used to obtain highly soluble PI to assure its processability for further used in films development.

In general, most insoluble aromatic PIs have been prepared as thin films through thermal imidization of polyamic acids (PAA) up to 300 - 350 °C (Hsiao & Chen 2002; Li & Hsu 2007). However, during this process, a controlled heating treatment is required, as rapid heating will lead to the formation of bubbles in the cast PAA layer, subsequently result in the failure of film production (Tan et al. 2017). In contrast, the formation of films from

organo-soluble PI could be performed at much lower temperatures, making it a more energy efficient process as it practically employs solvent evaporation technique (Alvino & Edelman 1978; Deng et al. 2018; Hasegawa, Fujii & Wada 2018). Since our goal is to produce organo-soluble PI, the second route is preferable.

Many previous studies concerning PIs film formation have focused on the diamine and dianhydride based monomers. However, little attention has been given to the other alternative monomers such as diisocyanate and dianhydride. This might be due to the fact that the aromatic PI obtained through these monomers is often in the form of powder, which may be insoluble, rendering a challenging film processing. Nevertheless, in comparison to diisocyanate, obtaining the organo-soluble PI powder from diamine requires a much more complicated process involving additional chemical reagents (Takekoshi 1996).

Therefore, the monomers used in PI synthesis should be carefully chosen for specific application requirements since it could affect the properties of the produced films. Due to the lack of research on the approaches for producing polyimide-based diisocyanate films, the present works aimed to evaluate the critical parameters for developing PI films involving 4,4'-methylene diphenyl diisocyanate (MDI) and 6FDA powder. The film fabrication optimization process for PI derived from these monomers has not yet been reported. In addition, the diversity of monomer combinations makes it impractical to have one universal film-forming process attributed to their different processability properties. The optical, mechanical, chemical resistance, crystallization and thermal properties of the obtained PI films are discussed.

## MATERIALS AND METHODS

## MATERIALS

6FDA (99%), MDI (98%), *N*-methyl-2-pyrrolidinone (NMP), *N,N*-dimethylformamide (DMF), *N,N*-dimethylacetamide (DMAc), tetrahydrofuran (THF), acetonitrile (ACN), were purchased from Sigma Aldrich Chemie GmbH, Germany. Dimethyl sulfoxide (DMSO), Dichloromethane (DCM), ethanol and methanol used were obtained from System, Malaysia, while acetone and chloroform (CHCl<sub>3</sub>) were from R&M chemical company, England. Standard Kapton film (film thickness: 24 μm) was from DuPont company. All chemicals were used as received, and all organic solvents were dried over an activated 4Å molecular sieve prior to use.

## MEASUREMENTS

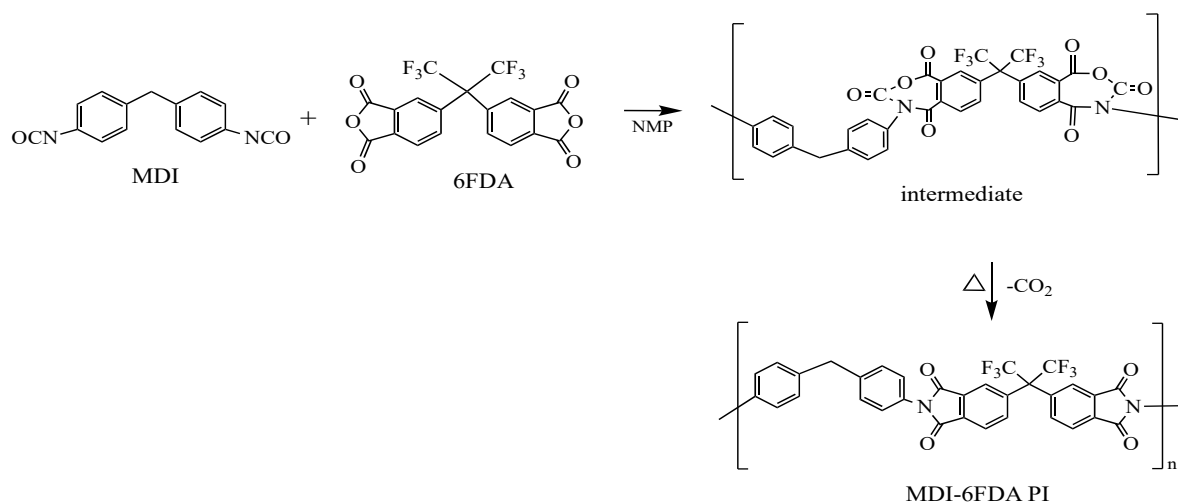
Fourier transform infrared (FTIR) spectrum of the powder sample was performed on Agilent Cary 630 spectrometer using diamond as the attenuated total reflectance (ATR) accessory. Nuclear magnetic resonance (NMR) measurement of the sample was carried out using Bruker Avance III HD 400 MHz spectrometer with dimethyl sulfoxide (DMSO)- $d_6$  as a solvent. The molecular weight of the polymer was measured via gel permeation chromatography (GPC) using Shodex GPC101 after calibrating with pullulan standard. The DMF/0.1M lithium bromide (LiBr) solution was used as an eluent for this measurement. The film thickness was measured on the Bruker DektakXT Standard System (DXT-S) surface profiler. The crystallinity of the films was determined using Bruker D8 Advance X-ray diffractometer with Cu- $k\alpha$  radiation ( $\alpha = 1.5406 \text{ \AA}$ ). A Perkin Elmer Lambda 35 spectrophotometer was used to measure the ultraviolet-visible (UV-vis) absorption spectra. Tensile properties of PI films (film dimension: 50 mm long, 10 mm wide) were characterized using a universal testing machine Shimadzu AGS-50KNX with a cross-head speed of 0.5 mm/min at room temperature. Differential scanning calorimetry (DSC) and thermogravimetric analysis (TGA) were conducted at a heating rate of 10 °C/min in nitrogen on NETZSCH DSC 214 Polyma calorimeter and PerkinElmer TGA 4000 analyzer, respectively. The chemical resistance of films was tested in 8 different solvents at ambient temperature for a maximum of 30 min.

## SYNTHESIS OF MDI-6FDA POLYIMIDE POWDER

The polymerization process was done in a glovebox under a high-purity nitrogen environment. A mixture of 10 mmol MDI and 10 mmol of 6FDA was reacted in NMP at ambient temperature for 15 min. After 15 min of stirring, the solution mixture was heated at 100 °C for 3.5 h. Then, the solution was left to cool and poured into a large amount of distilled water to obtain the precipitated PI powder. The resulting product was filtered, washed with methanol, and dried at 100 °C for 5 h in a vacuum oven. The reaction is shown in Scheme 1. The MDI-6FDA PI (yield: 95.5%) structure was confirmed using IR and NMR analysis.

## PREPARATION OF MDI-6FDA POLYIMIDE FILMS

A solvent casting technique was used to develop MDI-6FDA PI film with different drying parameters. MDI-6FDA PI solution at 15% solid concentration in DMAc was prepared and filtered through a 0.45  $\mu\text{m}$  filter syringe in an ambient atmosphere. The filtered solution was drop-cast onto a glass slide (dimensions: 23 mm wide  $\times$  38 mm long) and dried using different drying methods, as summarised in Table 1. It should be noted that a direct drying procedure was used. The number of solution drops was also evaluated in order to get a uniform colour and film thickness. The total number of drops examined was 26, 33, 35, and 46. The quantity of drops is governed by the surface tension of the solution. A commercialised PI film, Kapton (Figure 1), of 24  $\mu\text{m}$  thick, was employed as a standard reference and characterised accordingly.



SCHEME 1. Synthesis of MDI-6FDA polyimide

TABLE 1. Drying test parameters for MDI-6FDA polyimide films

Drying method	Temperature (°C)	Drying time (h)
Fume hood	Ambient	24
Glovebox	Ambient	24
Drying oven	60	2
	80	
	90	
	100	
Vacuum oven	80	2
	100	
	160	

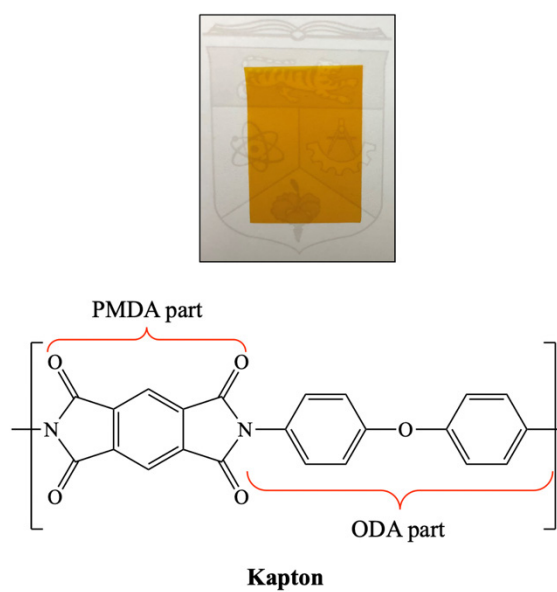


FIGURE 1. The films and structure of Kapton made up of pyromellitic dianhydride (PMDA) and 4,4'-oxydianiline (ODA)

## RESULTS AND DISCUSSION

## MDI-6FDA POLYIMIDE POWDER

The presence of peaks at  $1366\text{ cm}^{-1}$  (C-N),  $1780\text{ cm}^{-1}$  (C=O asymmetric),  $1719\text{ cm}^{-1}$  (C=O symmetric),  $1508\text{ cm}^{-1}$  (C=C),  $721\text{ cm}^{-1}$  (C=O bending), and  $1252\text{ cm}^{-1}$  ( $\text{CF}_3$ ) in the IR spectrum indicates the completion of the polymerization reaction. The IR spectrum of synthesised powder have been discussed in the previous study (Mustaffa et al. 2022). Further confirmation was obtained through  $^1\text{H-NMR}$  and  $^{13}\text{C-NMR}$  analyses, with the following peaks observed in the  $^1\text{H-NMR}$  spectrum (400 MHz,  $\text{DMSO-}d_6$ ,  $\delta$ , ppm): 7.35-7.44 (H1-H2), 4.08 (H3), 7.74-8.16 (H4-H6), while peaks in  $^{13}\text{C NMR}$  spectrum (400 MHz,  $\text{DMSO-}d_6$ ,  $\delta$ , ppm): 120.1-146.7 (C1-C4, C7-C12), 40.8 (C5), 166.7 (C6), 64.9 (C13), 109.8 (C14) (Mustaffa et al. 2022). Based on our previous study (Mustaffa et al. 2022), both NMR spectra exhibited peaks corresponding to proton and carbon signals of NMP residue, indicating that strong interactions between PI and NMP make it challenging to entirely extract the solvent from the MDI-6FDA PI products (Barsema et al. 2004; Kaba et al. 2005). This will be taken into account throughout the solvent evaporation process for film development. MDI-6FDA PI powder are highly soluble in NMP, DMSO, DMF, DMAc and THF. The obtained MDI-

6FDA PI has a weight average molecular weight ( $M_w$ ) of 35.6 kg/mol, number average molecular weight ( $M_n$ ) of 26.8 kg/mol and polydispersity index (PDI) of 1.33.

## FILMS DEVELOPMENT

Figure 2 depicts the physical state of MDI-6FDA PI film formation under various drying conditions. The drying method and temperature were designed in stages, from ambient to heating in vacuum atmosphere up to  $160\text{ }^\circ\text{C}$ , which is close to the solvent evaporation temperature (DMAc:  $165\text{ }^\circ\text{C}$ ; NMP:  $202\text{ }^\circ\text{C}$ ). Based on the observation, the MDI-6FDA films in Figure 2(a) to 2(h) are brittle and break before being removed from the glass slide, except for MDI-6FDA film (i).

Figure 2(a) shows that evaporating the solvent in an ambient environment is not a viable method for producing a film. It can be seen that it retains the characteristics and texture of the powder due to the reaction of moisture in the fume hood environment with the solvent, and thus reproduces the MDI-6FDA powder. Furthermore, despite the introduction of an inert environment for the drying of the solution in the glove box (method (b)), the room temperature used was insufficient for solvent evaporation to form a film. This causes only the moisture in the solvent to evaporate, leaving a fine yellowish powdery texture on the MDI-6FDA film, as shown in Figure 2(b).

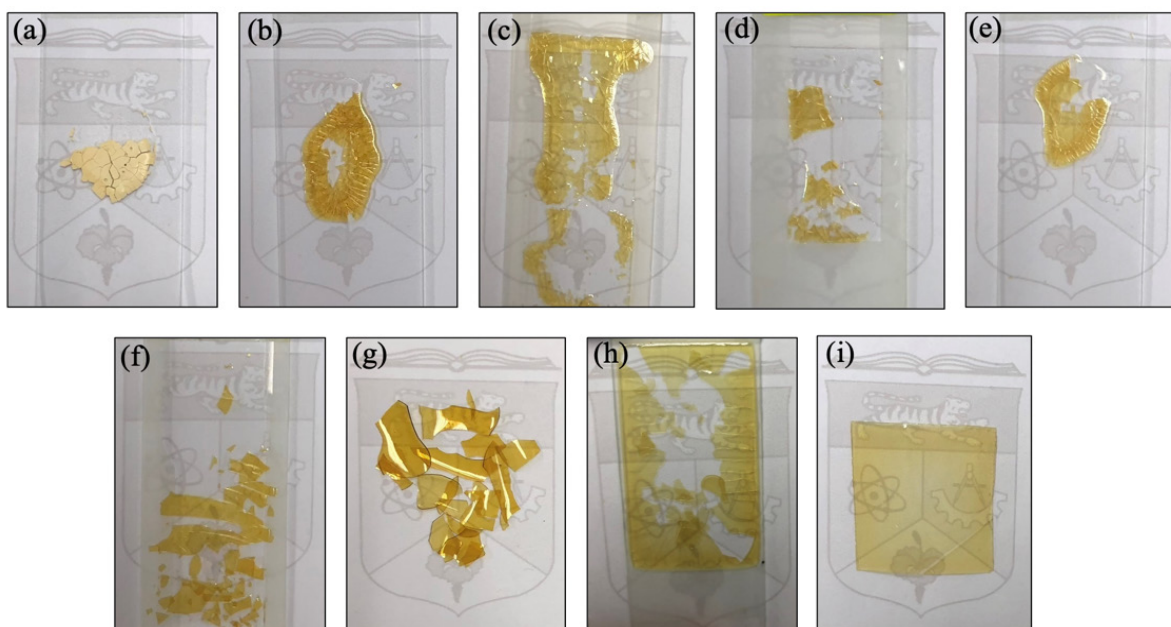


FIGURE 2. MDI-6FDA PI films after drying in various parameter. (a) Fume hood (24 h); (b) Glovebox (24 h); (c) Drying oven ( $60\text{ }^\circ\text{C}$ , 2 h); (d) Drying oven ( $80\text{ }^\circ\text{C}$ , 2 h); (e) Drying oven ( $90\text{ }^\circ\text{C}$ , 2 h); (f) Drying oven ( $100\text{ }^\circ\text{C}$ , 2 h); (g) Vacuum oven ( $80\text{ }^\circ\text{C}$ , 2 h); (h) Vacuum oven ( $100\text{ }^\circ\text{C}$ , 2 h); (i) Vacuum oven ( $160\text{ }^\circ\text{C}$ , 2 h)

Meanwhile, a better MDI-6FDA film texture was achieved through an oven-based film drying process (Figure 2(c) - 2(i)). However, heating the film in a drying oven (Figure 2(c) - 2(f)) has resulted in a film that is significantly more brittle than film dried in a vacuum oven. When removed from the glass slides, films produced in a vacuum oven are less likely to shatter than films from the conventional ovens. This could be due to a lack of moisture, that had been removed under vacuum (Reis 2014), which helps to increase the drying rate and results in a firmer film texture (Jiang, Zhang & Adhikari 2013; Punathil & Basak 2016). Furthermore, vacuum drying causes more evaporation of solvent in less drying time than conventional drying ovens (Ngamwonglumlert & Devahastin 2018).

Generally, a flexible and non-brittle MDI-6FDA film (i) is successfully obtained by drying under vacuum at 160 °C for 2 h. The high temperature required to eliminate excess solvent for flexible film formation may be due to the presence of NMP solvent traces in the polymer (Alvino & Edelman 1978), as supported by the NMR analysis.



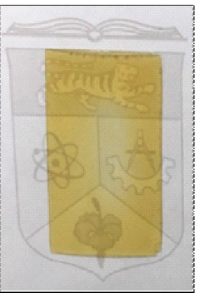

In addition, Table 2 further shows that the thickness and colour homogeneity of the MDI-6FDA film were affected by the volume of solution droplets. According to the table, 46 drops (1 mL) of solution could produce a film with a uniform colour and average thickness across the surface, which also indicates sufficient surface tension for the size of the film sample tested in this study. On the other hand, a thinner surface results in a film with

a brighter and more transparent colour in the center of the films with 26, 33, and 35 total drops of solution. The average thickness of the film surface indirectly influences the colour homogeneity of the MDI-6FDA film. Nonetheless, film with uniform colour and surface thickness (46 drops) is essential for practical use. The properties of the MDI-6FDA film were examined by employing a commercial Kapton (Figure 1) as a standard reference film

#### X-RAY DIFFRACTION (XRD) ANALYSIS

Figure 3 illustrates the X-ray diffractograms of the obtained MDI-6FDA film and standard Kapton. A distinct pattern of peak reflection was observed at  $2\theta = 10^{\circ}$ – $37^{\circ}$  attributed to the different polymer structure of these two PI films. Kapton film has a slightly higher degree of crystallinity than MDI-6FDA film due to its rigid PMDA structure (Hsiao & Chen 2002; Hsiao & Lin 2005). Nevertheless, both PI films exhibit broad diffraction peaks, indicating less crystalline polymer characteristics. The flexible ether and  $\text{CF}_3$  groups in Kapton and MDI-6FDA, respectively, have increased the free chain rotation and disrupted the structural regularity of the polymer film (Ando, Matsuura & Sasaki 1997; Cao et al. 2016; Huo et al. 2012). This observation was also evidenced by the DSC study, where no obvious melting point peak was found in the spectra of either MDI-6FDA or Kapton film.

TABLE 2. Drop test for MDI-6FDA PI film (i)

Total drops	26	33	35	46
Film samples (23 mm × 38 mm)				
<sup>a</sup> Thickness (μm)	92	94	94	93
<sup>b</sup> Thickness (μm)	69	67	70	-

<sup>a</sup> Average thickness of the film sides; <sup>b</sup> Average thickness of the centre area of the film

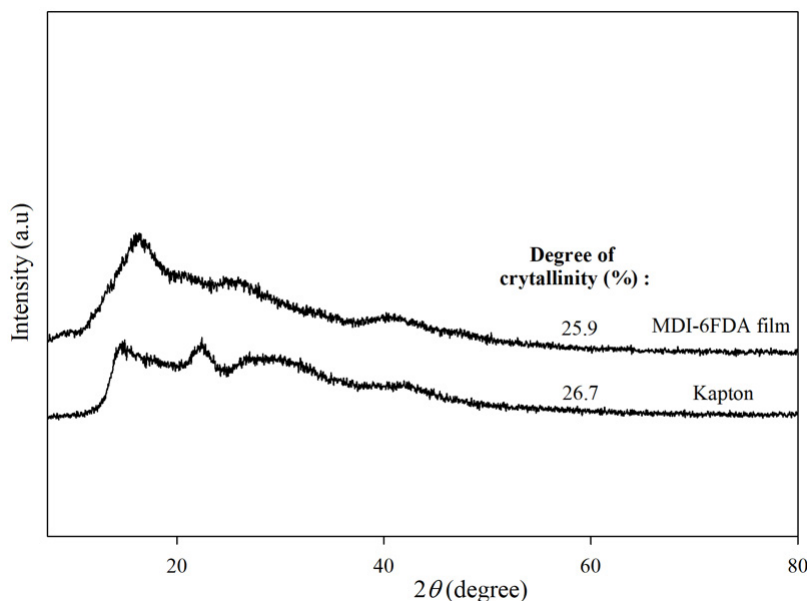


FIGURE 3. X-ray diffractogram of PI films

#### OPTICAL PROPERTIES

Table 3 shows the cut-off wavelength and optical transmittance at 500 nm obtained from the UV-vis spectra (Figure 4). The transmission cut-off measured at 500 nm of visible wavelength, corresponds to the maximum intensity of solar radiation (Kambezidis 2012). The large difference in the transparency value of both PI films was strongly influenced by the differences in their polymer structure. Based on Table 3, MDI-6FDA film exhibits good transparency properties with a higher light transmission value than that of Kapton film. This is due to the steric hindrance from the large  $C(CF_3)_2$  group in MDI-6FDA film has prevented the formation of intermolecular CT interactions, resulting in a film with a less intense colour than Kapton film (Ando, Matsuura & Sasaki 1997; Ghosh, Mistri & Banerjee 2015; Hasegawa & Horie 2001; St Clair, St Clair & Shevket 1984). Meanwhile, the rigid conjugated PMDA structure on Kapton has enhanced the interactions between molecules in the polymer and led to the intense brown film colour (Ando, Matsuura & Sasaki 1997; Deng et al. 2018). This in turn produces a higher light absorption of Kapton film in the violet-blue region (400 nm - 490 nm) compared to MDI-6FDA film (Shen, Feng & Zhang 2020). This finding highlights the potential advantage of MDI-6FDA film for use in optical application.

#### MECHANICAL PROPERTIES

The mechanical properties of the two PI films determined from the stress-strain curves (Figure 5) are listed in Table 4. The presence of bridging dianhydride and flexible  $CF_3$  in MDI-6FDA film reduces the rigidity of the polymer chain, resulting in lower tensile strength and modulus when compared to Kapton with stiff and non-bridging dianhydride (Liaw et al. 2012; Liu et al. 2012). Besides, the large  $C(CF_3)_2$  bridging in MDI-6FDA film has also increased the steric hindrance between the chains, thus inhibiting interactions between molecules in the polymer (Liu et al. 2012). This also supports the higher transparency of MDI-6FDA film over Kapton film. However, both PI films show good film flexibility, with up to 5% elongation at break. The mechanical properties of both PI films are comparable to PET and PEN polymer films, which are commonly used as flexible substrates with a tensile strength of 52 MPa and 82 MPa, respectively (Lim et al. 2012).

#### THERMAL PROPERTIES OF PI FILM

Figures 6 and 7 represent TGA and DSC thermograms of PI films, respectively. Noticeably, the decomposition peak at 360 °C in Figure 6 for MDI-6FDA film corresponds to the decomposition of trace amounts of

solvent in the sample. According to Table 5, MDI-6FDA film demonstrates excellent thermal stability at 674 °C in a nitrogen atmosphere, comparable to reference film Kapton. However, the  $T_g$  value of MDI-6FDA film is lower at 238 °C compared to Kapton film. This is because the presence of a large  $CF_3$  group in 6FDA has increased the intermolecular spacing between the chains, resulting in a lower packing density and rigidity of the polymer compared to PMDA in Kapton (Hu et al. 2021; Huang et al. 2017). This enables the polymer chains to move more easily and with less energy (Peng, Dussan & Narain 2020; Shrivastava 2018), producing a lower  $T_g$  temperature in MDI-6FDA film than in Kapton. Despite this, the  $T_g$  of the MDI-6FDA film achieved in this study is comparable to the  $T_g$  of the PI film structure from the previous study with the  $C(CF_3)_2$  group (Jang et al. 2007). Although the  $CF_3$  structural features have helped to improve the transparency of MDI-6FDA film (Table 3) by reducing the rigidity of the polymer chain (Ando, Matsuura & Sasaki 1997), it has also significantly reduced its thermal resistance.

#### CHEMICAL RESISTIVITY OF FILMS

The chemical resistivity of both PI films was tested in several solvents. Aromatic PIs typically have good

chemical resistivity but poor solubility in organic solvents (Vivod et al. 2020) due to their strong, rigid conjugated structure and intermolecular forces (Hu et al. 2021). As shown in Table 6, no discernible changes can be seen on the reference film Kapton in all tested solvents due to its stiff conjugated PMDA structure (Yi et al. 2020). However, MDI-6FDA film exhibits relatively lower chemical stability to solvents tested, such as acetone,  $CH_3CN$ , DCM and  $CH_2Cl_2$ , than Kapton film. This could be attributed to the bulky and flexible  $C(CF_3)_2$  bridging groups at the aromatic MDI-6FDA backbone, which disrupted the tight stacking of the polymer chains and weakened the intermolecular interactions (Hu et al. 2021; Huang et al. 2019), making it less rigid than the Kapton film. The less rigid polymer structure of MDI-6FDA film has reduced its durability and chemical stability (Vivod et al. 2020). In general, for practical use, the chemical environment or solvent involved in the intended application must be considered to ensure the stability of the obtained MDI-6FDA film. For example, when used as a substrate in dye-sensitized solar cells, an alternative electrolyte solvent such as ethanol should be considered rather than  $CH_3CN$  solvent (An et al. 2006; Xue et al. 2004).

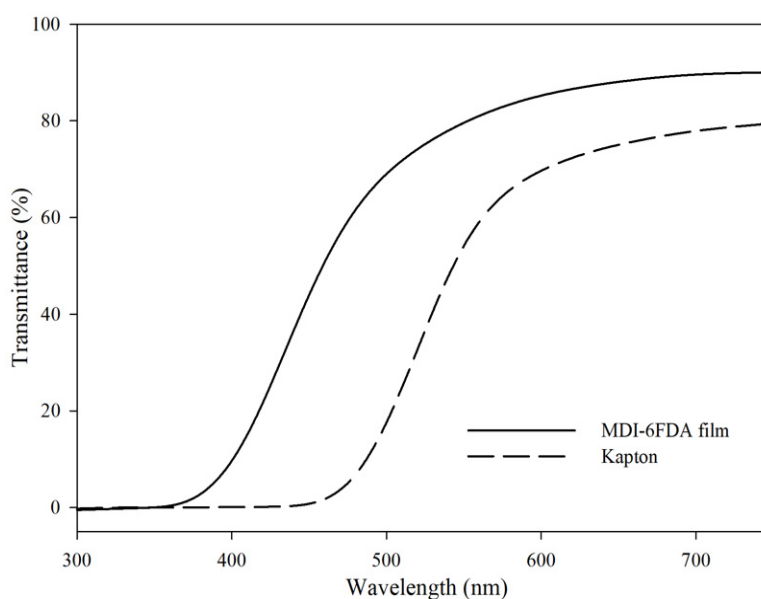


FIGURE 4. Transmittance of the films



TABLE 3. Optical properties of PI films

Film sample	$\lambda_0^a$ (nm)	Kehantaran <sup>b</sup> (%)
MDI-6FDA	371	69
Kapton	453	18

<sup>a</sup>Cut-off wavelength (absorption edge,  $\lambda_0$ ), <sup>b</sup>Transmittance at 500 nm (%)

TABLE 4. Mechanical properties of the PI films

Film sample	Tensile strength (MPa)	Modulus (GPa)	Elongation at break (%)
MDI-6FDA	$57 \pm 4.2^*$	$1.6 \pm 0.21^*$	$5 \pm 0.49^*$
Kapton	$84 \pm 2.8^*$	$3.5 \pm 0.14^*$	$5 \pm 0.28^*$

\*Standard deviation

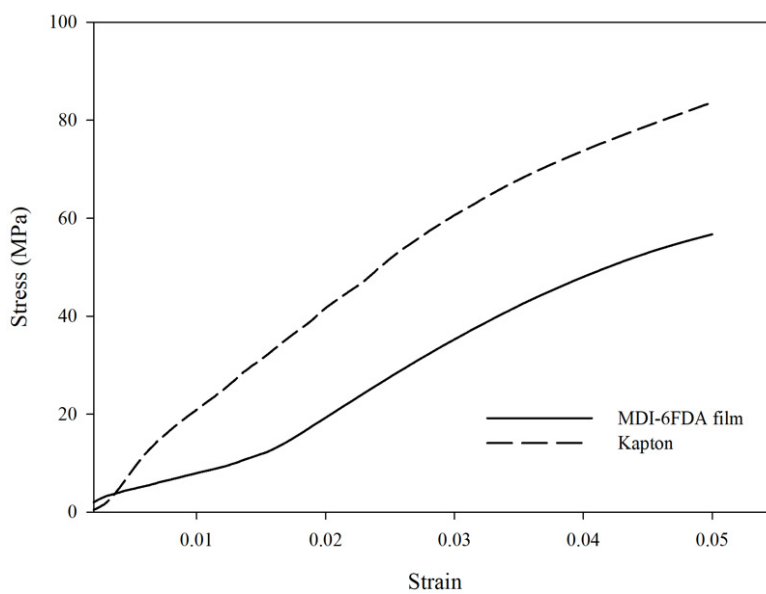


FIGURE 5. Stress-strain curves

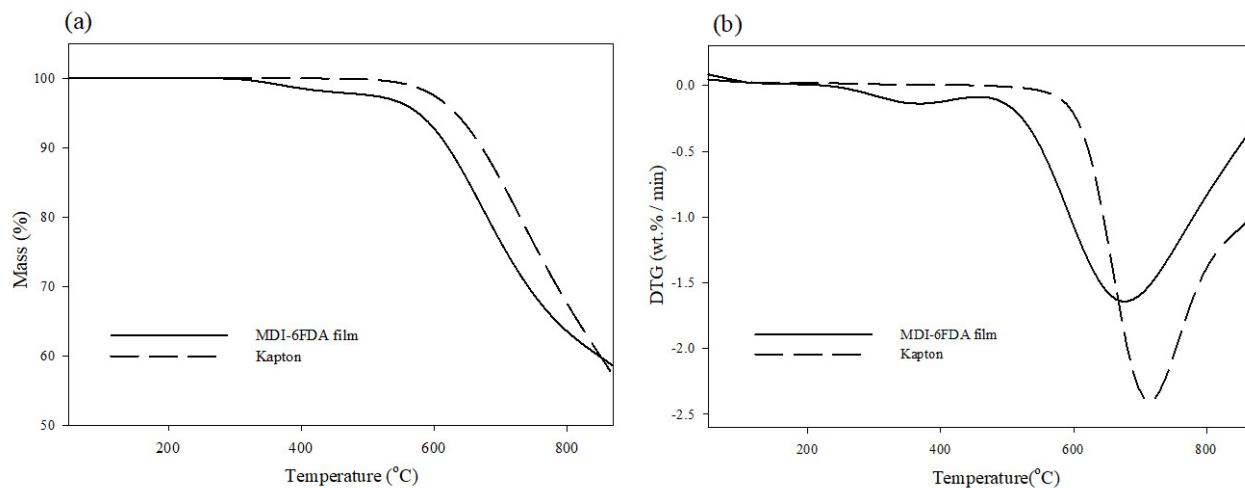


FIGURE 6. Thermal stability of polyimide (a) TGA thermogram (b) DTG curves of PI films

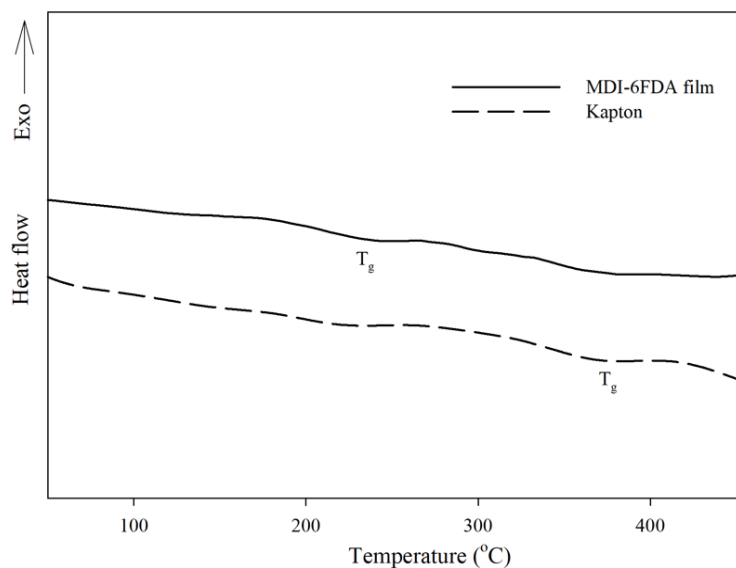


FIGURE 7. DSC curves of PI films

TABLE 5. Thermal properties of PI films

Film sample	$T_g$ (°C) <sup>a</sup>	$T_5$ (°C) <sup>b</sup>	$T_{10}$ (°C) <sup>c</sup>	$T_{max}$ (°C) <sup>d</sup>
MDI-6FDA	238	574	623	674
Kapton	378	647	680	713

<sup>a</sup>Glass transition temperature from DSC measurement; <sup>b</sup>Temperature at 5% weight loss recorded by TGA analysis; <sup>c</sup>Temperature at 10% weight loss recorded by TGA analysis; <sup>d</sup>Maximum degradation temperature from DTG thermogram

TABLE 6. Chemical resistivity of PI films

Film sample <sup>a</sup>	Organic solvents							
	Acetone	Methanol	Ethanol	Isopropanol	THF	CH <sub>3</sub> CN	DCM	CH <sub>3</sub> Cl
MDI-6FDA	+	-	-	-	-	+	++	-*
Kapton	-	-	-	-	-	-	-	-

(-): No physical change, (+): Film breaking, (++): Film dissolve completely, (-\*): Film degrade, but not breaking

<sup>a</sup>Film dimension of (5 × 5) mm

### CONCLUSION

A flexible MDI-6FDA film with an average thickness of 93  $\mu\text{m}$  was successfully developed by casting 46 drops (1 mL) of solution and drying for 2 h in a vacuum oven at 160 °C. The resulting film has a tensile strength of up to 57 MPa with an elongation at break of 5%. The incorporation of large CF<sub>3</sub> bridging groups has reduced the rigidity of the polymer chain, hence indirectly affecting the mechanical properties of the MDI-6FDA film. Nonetheless, the polymer structure of the MDI-6FDA film has contributed to a better light transmission of up to 69% at 500 nm compared to 18% for standard reference film Kapton. This has become one of the appealing properties of the flexible MDI-6FDA PI film developed in this study, which potentially used in optical applications. In addition, the obtained MDI-6FDA film demonstrates excellent thermal resistance ( $T_5 = 574$  °C) with a  $T_g$  temperature of up to 238 °C.

### ACKNOWLEDGEMENTS

This research is financially supported by the Fundamental Research Grant Scheme, (FRGS/1/2018/STG01/UKM/02/16). The authors would like to thank the Faculty of Science and Technology (FST) of Universiti Kebangsaan Malaysia (UKM), specifically, the Department of Chemical Sciences (JSK) and Polymer Research Centre (PORCE) for technical support and facilities given. The authors acknowledge the Centre for Research and Instrument Management (CRIM), UKM for the support in sample characterization (XRD).

### REFERENCES

Alvino, W.M. & Edelman, L.E. 1978. Polyimides from diisocyanates, dianhydrides, and their dialkyl esters. *Journal of Applied Polymer Science* 22(7): 1983-1990.

- Amutha, N., Tharakan, S.A. & Sarojadevi, M. 2015. Synthesis and characterization of new soluble polyimides based on pyridine unit with flexible linkages. *High Performance Polymers* 27(8): 979-989.
- An, H., Xue, B., Li, D., Li, H., Meng, Q., Guo, L. & Chen, L. 2006. Environmentally friendly Lil/ethanol based gel electrolyte for dye-sensitized solar cells. *Electrochemistry Communications* 8(1): 170-172.
- Ando, S., Matsuura, T. & Sasaki, S. 1997. Coloration of aromatic polyimides and electronic properties of their source materials. *Polymer Journal* 29(1): 69-76.
- Barsema, J.N., Klijnsstra, S.D., Balster, J.H., Van der veegt, N.F.A., Koops, G.H. & Wessling, M. 2004. Intermediate polymer to carbon gas separation membranes based on Matrimid PI. *Journal of Membrane Science* 238(1-2): 93-102.
- Cao, L., Zhang, M., Niu, H., Chang, J., Liu, W., Yang, H., Cao, W. & Wu, D. 2016. Structural relationship between random copolyimides and their carbon fibers. *Journal of Materials Science* 52(4): 1883-1897.
- Deng, B., Zhang, S., Liu, C., Li, W., Zhang, X., Wei, H. & Gong, C. 2018. Synthesis and properties of soluble aromatic polyimides from novel 4,5-diazafuorene-containing dianhydride. *RSC Advances* 8(1): 194-205.
- Ghosh, A., Mistri, E.A. & Banerjee, S. 2015. Fluorinated polyimides: Synthesis, properties, and applications. *Handbook of Specialty Fluorinated Polymers*. pp. 97-185.
- Hasegawa, M., Fujii, M. & Wada, Y. 2018. Approaches to improve the film ductility of colorless cycloaliphatic polyimides. *Polymers for Advanced Technologies* 29(2): 921-933.
- Hasegawa, M. & Horie, K. 2001. Photophysics, photochemistry, and optical properties of polyimides. *Progress in Polymer Science* 26(2): 259-335.
- Hsiao, S.H. & Chen, Y.J. 2002. Structure-property study of polyimides derived from PMDA and BPDA dianhydrides with structurally different diamines. *European Polymer Journal* 38(4): 815-828.

- Hsiao, S.H. & Lin, K.H. 2005. Polyimides derived from novel asymmetric ether diamine. *Journal of Polymer Science Part A: Polymer Chemistry* 43(2): 331-341.
- Hu, M., Chen, H., Wang, M., Liu, G., Chen, C., Qian, G. & Yu, Y. 2021. Novel low-dielectric constant and soluble polyimides from diamines containing fluorene and pyridine unit. *Journal of Polymer Science* 59(4): 329-339.
- Huang, X., Li, H., Liu, C. & Wei, C. 2019. Design and synthesis of high heat-resistant, soluble, and hydrophobic fluorinated polyimides containing pyridine and trifluoromethylthiophenyl units. *High Performance Polymers* 31(1): 107-115.
- Huang, X., Chen, B., Mei, M., Li, H., Liu, C. & Wei, C. 2017. Synthesis and characterization of organosoluble, thermal stable and hydrophobic polyimides derived from 4-(4-(1-pyrrolidiny)phenyl)-2,6-bis(4-(4-aminophenoxy)phenyl)pyridine. *Polymers* 9(10): 1-13.
- Huo, H., Mo, S., Sun, H., Yang, S. & Fan, L. 2012. Preparation and properties of molecular-weight-controlled polyimide adhesive film. *e-Polymers* 12(1): 1-18.
- Hyde, L.J. & Smith, R.M. 1995. Bearing-grade thermoplastic polyimides in automotive tribological applications. (No. 950190) *SAE Technical Paper* pp. 1-11.
- Jang, W., Shin, D., Choi, S., Park, S. & Han, H. 2007. Effects of internal linkage groups of fluorinated diamine on the optical and dielectric properties of polyimide thin films. *Polymer* 48(7): 2130-2143.
- Jiang, H., Zhang, M. & Adhikari, B. 2013. Fruit and vegetable powders. *Handbook of Food Powders*. Elsevier. pp. 532-552.
- Kaba, M., Romero, R.E., Essamri, A. & Mas, A. 2005. Synthesis and characterization of fluorinated copolyetherimides with  $\text{CH}_2\text{C}_6\text{F}_{13}$  side chains based on the ULTEM™ structure. *Journal of Fluorine Chemistry* 126(11-12): 1476-1486.
- Kambezidis, H.D. 2012. The solar resource. *Comprehensive Renewable Energy* 3: 27-84.
- Li, T.L. & Hsu, S.L.C. 2007. Preparation and properties of a high temperature, flexible and colorless ITO coated polyimide substrate. *European Polymer Journal* 43(8): 3368-3373.
- Liaw, D.J., Huang, C.C. & Chen, W.H. 2006. Color lightness and highly organosoluble fluorinated polyamides, polyimides and poly(amide-imide)s based on noncoplanar 2,2'-dimethyl-4,4'-biphenylene units. *Polymer* 47(7): 2337-2348.
- Liaw, D.J., Wang, K.L., Huang, Y.C., Lee, K.R., Lai, J.Y. & Ha, C.S. 2012. Advanced polyimide materials: Syntheses, physical properties and applications. *Progress in Polymer Science* 37(7): 907-974.
- Lim, C.Y., Park, J.K., Kim, Y.H. & Han, J.I. 2012. Mechanical and electrical stability indium-tin-oxide coated polymer substrates under continuous bending stress condition. *Journal of International Council on Electrical Engineering* 2(3): 237-241.
- Liu, J., Zhang, Q., Xia, Q., Dong, J. & Xu, Q. 2012. Synthesis, characterization and properties of polyimides derived from a symmetrical diamine containing bis-benzimidazole rings. *Polymer Degradation and Stability* 97(6): 987-994.
- Mustaffa, N., Kaneko, T., Takada, K., Dwivedi, S., Su'ait, M.S. & Mobarak, N.N. 2022. Synthesis and characterization of polyimides from diisocyanate with enhanced solubility and thermostability properties via direct low-temperature one-step polymerization in NMP solvent. *Polymer Bulletin*. pp. 1-17.
- Ngamwonglumlert, L. & Devahastin, S. 2018. Microstructure and its relationship with quality and storage stability of dried foods. *Food Microstructure and Its Relationship with Quality and Stability*. Elsevier. pp. 139-159.
- Peng, Y.Y., Dussan, D.D. & Narain, R. 2020. Thermal, mechanical, and electrical properties. *Polymer Science and Nanotechnology*. Elsevier. pp. 179-201.
- Punathil, L. & Basak, T. 2016. Microwave processing of frozen and packaged food materials: Experimental. *Reference Module in Food Science*. Elsevier. pp. 1-28.
- Qu, W., Ko, T.M., Vora, R.H. & Chung, T.S. 2001. Effect of polyimides with different ratios of para - to meta - analogous fluorinated diamines on relaxation process. *Polymer* 42(15): 6393-6401.
- Reis, F.R. 2014. Introduction to low pressure processes. In *Vacuum Drying for Extending Food Shelf-Life*, edited by Reis, F.R. Springer. pp. 1-6.
- Sadavarte, N.V., Halhalli, M.R., Avadhani, C.V. & Wadgaonkar, P.P. 2009. Synthesis and characterization of new polyimides containing pendent pentadecyl chains. *European Polymer Journal* 45(2): 582-589.
- Shen, Y., Feng, Z. & Zhang, H. 2020. Study of indium tin oxide films deposited on colorless polyimide film by magnetron sputtering. *Materials & Design* 193: 1-7.
- Shrivastava, A. 2018. *Introduction to Plastics Engineering*. Elsevier. pp. 1-16.
- St Clair, A.K., St Clair, T.L. & Shevket, K.I. 1984. Synthesis and characterization of essentially colorless polyimide films. *Journal of Polymer Material Science Engineering* 51: 62-66.
- Takekoshi, T. 1996. Synthesis of polyimides. In *Polyimides: Fundamentals and Applications*, edited by Ghosh, M. Boca Raton: CRC Press: pp. 7-48.
- Tan, P.C., Ooi, B.S., Ahmad, A.L. & Low, S.C. 2017. Correlating the synthesis protocol of aromatic polyimide film with the properties of polyamic acid precursor. *IOP Conference Series: Materials Science and Engineering* 206: 1-11.
- Tapaswi, P.K. & Ha, C.S. 2019. Recent trends on transparent colorless polyimides with balanced thermal and optical properties: Design and synthesis. *Macromolecular Chemistry and Physics* 220(3): 1-33.

- Thiruvassagam, P., Saritha, B. & Hari, N. 2016. Poly(ether-imide)s with flexible linkages and kinks: Synthesis, processability, thermal stability, and dielectric studies. *High Performance Polymers* 28(6): 660-668.
- Vivod, S.L., Meador, M.A.B., Pugh, C., Wilkosz, M., Calomino, K. & McCorkle, L. 2020. Toward improved optical transparency of polyimide aerogels. *ACS Applied Materials & Interfaces* 12(7): 8622-8633.
- Wu, H.W., Li, H. & Liu, H.Z. 2012. Synthesis and properties of a high-molecular-weight polyimide based on 4, 4'-(hexafluoroisopropylidene) diphthalic anhydride. *Advanced Materials Research* 550-553: 742-746.
- Xue, B.F., Wang, H.X., Hu, Y.S., Li, H., Wang, Z.X., Meng, Q.B., Huang, X.J., Sato, O., Chen, L.Q. & Fujishima, A. 2004. An alternative ionic liquid based electrolyte for dye-sensitized solar cells. *Photochemical & Photobiological Sciences* 3(10): 918-919.
- Yi, C., Li, W., Shi, S., He, K., Ma, P., Chen, M. & Yang, C. 2020. High-temperature-resistant and colorless polyimide: Preparations, properties, and applications. *Solar Energy* 195: 340-354.

\*Corresponding author; email: nadhratunnaiim@ukm.edu.my